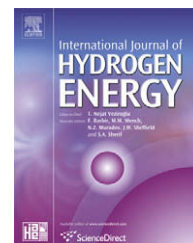


Available at www.sciencedirect.comjournal homepage: www.elsevier.com/locate/he

Hydrogen purification using compact pressure swing adsorption system for fuel cell

Edy Herianto Majlan^{a,*}, Wan Ramli Wan Daud^a, Sunny E. Iyuke^b,
Abu Bakar Mohamad^c, A. Amir H. Kadhum^c, Abdul Wahab Mohammad^c,
Mohd. Sobri Takriff^c, Nurhaswani Bahaman^a

^aFuel Cell Institute, Universiti Kebangsaan Malaysia, 43600 Bangi, Selangor DE, Malaysia

^bSchool of Chemical and Metallurgical Engineering, University of the Witwatersrand, Johannesburg, South Africa

^cChemical and Process Engineering Dept., Faculty of Engineering, Universiti Kebangsaan Malaysia, 43600 Bangi, Selangor DE, Malaysia

ARTICLE INFO

Article history:

Received 4 September 2008

Received in revised form

19 December 2008

Accepted 23 December 2008

Available online 20 February 2009

Keywords:

Adsorption

Hydrogen purification

Activated carbon

Fuel cell

CPSA

PEMFC

Gas separation

ABSTRACT

Adsorption of CO and CO₂ in mixtures of H₂/CO/CO₂ was achieved using compact pressure swing adsorption (CPSA) system to produce purified hydrogen for use in fuel cell. A CPSA system was designed by combining four adsorption beds that simultaneously operate at different processes in the pressure swing adsorption (PSA) process cycle. The overall diameter of the cylindrical shell of the CPSA is 35 cm and its height is 40 cm. Several suitable adsorbent materials for CO and CO₂ adsorption in a hydrogen stream were identified and their adsorption properties were tested. Activated carbon from Sigma-Aldrich was the adsorbent chosen. It has a surface area of 695.07 m²/g. CO adsorption capacity (STP) of 0.55 mmol/g and CO₂ at 2.05 mmol/g were obtained. The CPSA system has a rapid process cycle that can supply hydrogen continuously without disruption by the regeneration process of the adsorbent. The process cycle in each column of the CPSA consists of pressurization, adsorption, blowdown and purging processes. CPSA is capable of reducing the CO concentration in a H₂/CO/CO₂ mixture from 4000 ppm to 1.4 ppm and the CO₂ concentration from 5% to 7.0 ppm CO₂ in 60 cycles and 3600 s. Based on the mixture used in the experimental work, the H₂ purity obtained was 99.999%, product throughput of 0.04 kg H₂/kg adsorbent with purge/feed ratio was 0.001 and vent loss/feed ratio was 0.02. It is therefore concluded that the CPSA system met the required specifications of hydrogen purity for fuel cell applications.

© 2009 International Association for Hydrogen Energy. Published by Elsevier Ltd. All rights reserved.

1. Introduction

Fuel cells are electrochemical devices that convert the chemical energy of a reaction directly into electrical energy, heat and water. The basic physical structure of a fuel cell consists of an electrolyte layer, which is in contact with a porous anode and cathode on either side. In a typical fuel cell, gaseous fuels are fed continuously to the anode (negative

electrode) and an oxidant (i.e., oxygen from air) is fed continuously to the cathode (positive electrode) [1]. Electrochemical reactions take place at the electrodes to produce electric current. Hydrogen is highly reactive when suitable catalysts are used, and thus becomes the choice of fuel in most applications of fuel cell. From an environmental point of view, hydrogen is the cleanest fuel known and it is expected that hydrogen technology will be able to revolutionize the

* Corresponding author. Tel.: +603 89216050; fax: +603 89216024.

E-mail address: edy@eng.ukm.my (E.H. Majlan).

transportation and energy market [2]. Hydrogen is also widely produced for chemical and industrial purposes by hydrogenation and methanol reforming to produce synthesis gas [3]. Hydrogen production currently relies on fossil fuels, using steam reforming of natural gas and coal gasification technologies [4]. Steam reformers often produce a small amount of carbon monoxide (typically 0.5–5 mol%). Carbon monoxide easily deactivates the catalyst of the proton exchange membrane fuel cell (PEMFC) electrode. Traces of carbon monoxide could cause detrimental effects on the cell voltage and reduce the fuel cell's power output [5]. A recent study indicates that approximately 10 ppm of CO in the feed gas stream of PEMFC reduces the cell performance [1]. Hence the carbon monoxide concentration needs to be reduced to a very low level, preferably below 10 ppm for the hydrogen-rich reformate effluent to be suitable as fuel cell feed.

In a case which requires high purity, the hydrogen product stream is passed on to a separation zone, which comprises a thermal swing adsorption system or a pressure swing adsorption (PSA) system to produce a high purity hydrogen stream (95–99.999 mol%) [3]. The PSA system is an adsorption system that can be used to purify H₂ from reformer effluent. The process cycle is fast, it can produce hydrogen continuously without disrupting the regeneration process of the used adsorbents. The PSA system allows one to give a purified hydrogen product at the same pressure of the feeding flow and at a high purity [6]. In a typical PSA cycle, the adsorbent is used for adsorption and regenerated several times before it loses its adsorptive capacity. The PSA system should have a compact design, small pressure drop and have to start the purification process instantaneously to ensure a continuous supply of clean H₂. Therefore, a compact pressure swing adsorption (CPSA) system was used to adsorb the CO and CO₂ from a model mixture of H₂/CO/CO₂, which was used in the study to mimic the steam reformer effluent whose moisture content has been removed by any standard process.

The main objective of this purification process is to remove or reduce the concentration of CO gas from the hydrogen stream to as low as 10 ppm or below. The reason for this objective is to produce pure hydrogen which can be used as fuel in PEMFC later on.

2. Material and experiment

2.1. Material and equipment

The CPSA system was designed according to White and Barkley [7]. The design was built based on: adsorption size, velocity, regeneration, and choice of the adsorbent material, specifications of which are presented in Table 1.

The compact design incorporates four beds in one cylinder, while the conventional design of PSA has a separate bed for each adsorber (Fig. 1).

The CPSA operates in five steps: (1) pressurization, (2) adsorption I (feed from previous bed), (3) adsorption II (direct feed), (4) blowdown, and (5) purging. On the other hand the PSA steps in the cycle process are run simultaneously whereas they are run intermittently on alternate adsorbers in a conventional PSA. For adsorption step in the CPSA system,

Table 1 – Specification of CPSA system.

Item	Parameter
CPSA Material	Stainless steel
CPSA Shape	Cylinder with four beds
Total bed height	30 cm
Total diameter of adsorption bed	35 cm
Adsorption pressure	5 atmosphere
Adsorption temperature	302.15 K
Concentration of CO in feed	4000 ppm
Concentration of CO ₂ in feed	5 mol%
Desorption pressure	1 atmosphere

feed for second bed is from product of first bed. Mixtures of hydrogen and CO will enter two beds in series before they exit from the CPSA. CO is adsorbed in the first and second beds, and purified hydrogen will exit through the CPSA as a product. The valves and process cycles control system were designed for manual and automatic operation.

The performance of the PSA cycle is measured in terms of three main parameters, namely, product impurity content, product recovery and product throughput. It should be noted that the term “product” in this work refers to the purified H₂ stream exiting the bed throughout the feed step (step 3). Product recovery manifests itself in two other parameters: purge/feed ratio and vent loss/feed ratio [8].

2.2. Experiment

CO adsorption was tested on three types of adsorbents, which are commercial activated carbon (AC), composite adsorbent and AC impregnated with Sn. Table 2 shows the adsorbents, which were used in the study.

The composite adsorbents used were modified original adsorbents (Table 1). The composite adsorbents were prepared according to Hirai et al [9]. A solution of copper (I) halide (concentration: 20–2000 mmol/l; color: pale yellow) in a solvent therefore was prepared. Examples of solvents of copper (I) halide are acetonitrile, methanol, ethanol, propionitrile, acetone, methyl ethyl ketone, methylene chloride, 1,2-dichloroethane, etc.

Pyridine compound is added from 0.2 to 5.0 mol per mole of copper (I) halide and the resultant mixture is stirred or shaken at 0–90 °C for 30 min–5 h. The color of the solution changed from pale yellow to yellow. This change indicates that the binary complex of the pyridine compound and copper (I) chloride was formed.

The above-obtained solution of binary complex was added to 1–100% by weight of the binary complex solution, of a porous inorganic carrier. The resultant mixture was stirred at 90 °C for 30 min–24 h. Subsequently, the solvent was removed under reduced pressure. Then the mixture was dried at 0–90 °C for 30 min–5 h under a pressure of 0.1–10 mmHg, thus, obtaining the pyridine compound/copper (I) halide binary complex–porous composite adsorbent. The modified composite adsorbents are the following:

- activated carbon composite: Sigma–Aldrich (AC-S-C);
- activated carbon composite: BDH Lab. (AC-BDH-C);

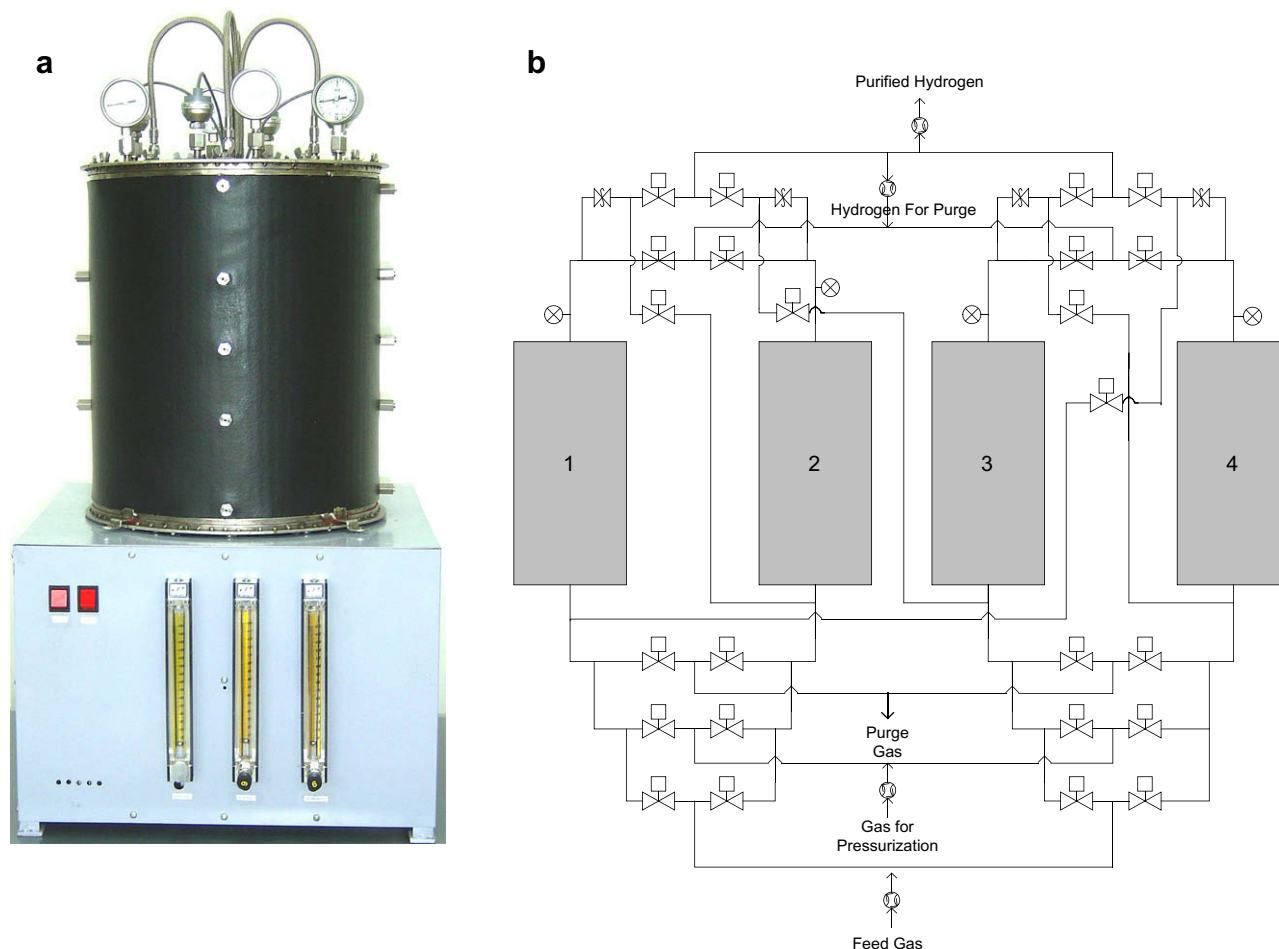


Fig. 1 – (a) CPSA system, (b) schematic CPSA.

- activated carbon composite: Mindong Lianyl (AC-H15-C);
- silica gel composite (SG-C).

Adsorbents impregnated with Sn were prepared according to the literature [10,11]. A known amount of $\text{SnCl}_2 \cdot 2\text{H}_2\text{O}$ (May and Baker) was dissolved in 40 ml of HCl and stirred under nitrogen. Four grams of AC were then added to the solution and agitated for 24 h under N_2 gas. The sample was then filtered and washed with distilled water until the pH of the water became around 5 and the sample was then dried at 200°C . The adsorbents impregnated with tin are as follows:

- activated carbon: BDH Lab. (AC-BDH-I);
- activated carbon: Mindong Lianyl (AC-H11-I);
- activated carbon: Mindong Lianyl (AC-H15-I).

The gases used were supplied by Malaysian Oxygen (MOX) Berhad. CO and nitrogen of purified grade gases are the adsorbates. Purified grade He was used as a carrier gas.

2.2.1. Analysis of adsorptive capacity of the adsorbent

The adsorbent capacity analysis was done by using the BET-AUTOSORB-1C equipment (Quanta Chrome Corp., USA). In this experiment, the temperature was set at 302 K and the pressure at 1 atm, for 360 s [10].

2.2.2. CO adsorption using CPSA

2.2.2.1. Single bed cycle. Adsorption was done on one bed while the other beds were regenerated or prepared for another adsorption process after the first bed saturated. The cyclic processes for every bed were: pressurization, adsorption process at high pressure, blowdown and purging. The single bed process cycle has been presented earlier by Iyuke et al [10].

Table 2 – Original adsorbents.

Adsorbent	Supplier	Particle size (mm)
Activated carbon (AC-S)	Sigma-Aldrich, Netherlands	0.84–2
Activated carbon (AC-BDH)	BDH Lab., UK	1–2
Activated carbon (C-H11)	Mindong Lianyl, China	1.68–2
Activated carbon (AC-H15)	Mindong Lianyl, China	1.19–1.41
Silica gel (SG)	Mindong Lianyl, China	1.68–2.38

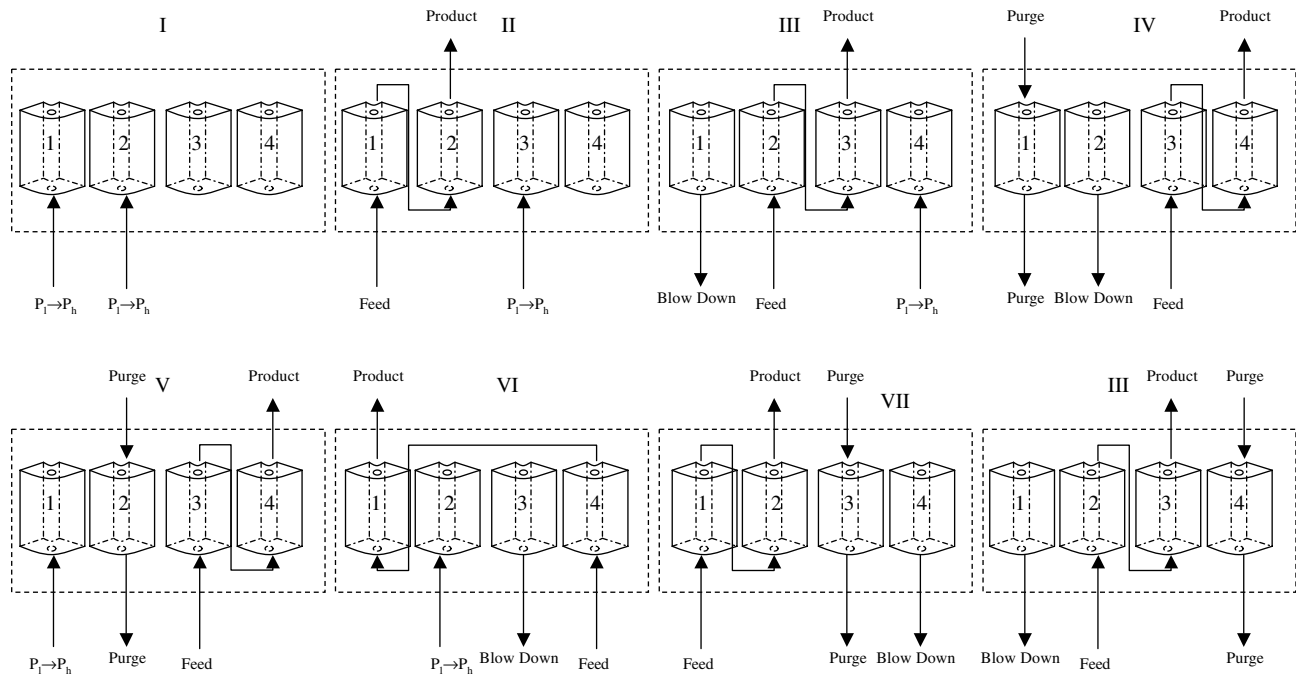


Fig. 2 – CPSA cyclic process for dual bed system (P_l : low pressure; P_h : high pressure).

2.2.2.2. *Dual bed cycle.* The dual bed process in the CPSA cycling system was an adsorption process which used two beds in series. At one time, there were two columns going through adsorption. The cyclic processes for every bed are listed below, as depicted in Fig. 2:

- pressurization;
- adsorption 1, feeder from the product of another column (refers to cycle II column 2, which receives feed from column 1) (Fig. 2);
- adsorption 2, feeder from the initial mixture gas (refers to cycle II column 1) (Fig. 2);

- blowdown;
- purging.

Non-dispersive infrared gas filter correlation, with solid state detector (7000FM – Signal UK), was used as the online CO and CO₂ analyzer.

3. Results and discussion

3.1. Choice of adsorbent

The adsorbent that was used in the hydrogen purification was chosen based on the adsorption capacity and the selectivity for CO. Table 3 shows the CO and CO₂ adsorption results using BET-AUTOSORB-1C for 360 s and the comparison of the adsorbent selectivity for CO. The adsorbent should have high

Table 3 – The capacity of the adsorbent in the CO and CO₂ adsorption process.

Adsorbent	CO adsorbed (mmol/g)	CO ₂ adsorbed (mmol/g)	CO/CO ₂ adsorbed
AC-S	0.13	0.15	0.87
AC-H15-C	0.05	0.17	0.32
SG-C	0.01	0.03	0.32
AC-BDH	0.13	0.51	0.26
AC-S-C	0.02	0.06	0.23
AC-BDH-C	0.04	0.20	0.20
AC-BDH-I	0.08	0.45	0.18
AC-H11-I	0.07	0.39	0.18
AC-H15-I	0.07	0.49	0.14
SG	0.02	0.16	0.11
AC-H15	0.06	0.62	0.09
AC-H11	0.04	0.45	0.08

Table 4 – Activated carbon (Sigma-Aldrich) characterization.

Specification	Result
Particle size	1–1.4 mm
Material	Charcoal
BET surface area	695.07 m ² /g
Micropore surface area	504.87 m ² /g
External micropore surface area	190.21 m ² /g
Micropore volume	0.210 ml/g
Average pore size	26.43 Å
Adsorption capacity of CO (STP)	0.55 mmol/g
Adsorption capacity of CO ₂ (STP)	2.05 mmol/g

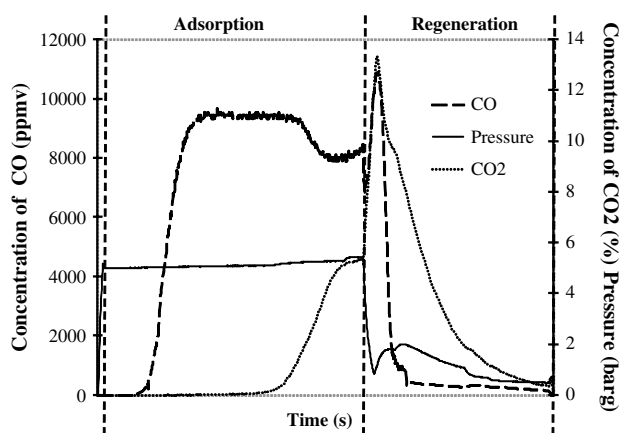


Fig. 3 – The pressure and concentration profile of CO–CO₂ in the product stream.

CO adsorption capacity and high selectivity for CO or the smallest selectivity for CO₂. Table 4 shows the data of activated carbon from Sigma–Aldrich. When the adsorption value of CO is larger compared to CO₂, the higher is the selectivity of the adsorbent to the CO and vice versa. From the adsorption capacity and selectivity results, Sigma–Aldrich (AC-S) was chosen as the adsorbent for the CPSA system to purify the hydrogen from H₂/CO/CO₂ mixtures.

3.2. CO–CO₂ adsorption process using the CPSA system

3.2.1. Single bed cycle

Fig. 3 shows the history of pressure and concentration of CO–CO₂ in the product stream. The concentration of CO in the feeder gas mixture was 4000 ppm and CO₂ was 5%. The flow rates of H₂, CO₂ and CO were 12,906 ml/min, 645 ml/min and 60 ml/min, respectively. Fig. 4 shows the CO and CO₂ concentration history in the product streams during the adsorption process.

From Fig. 4, it can be seen that CO was detected faster compared to CO₂ in the hydrogen product, which was produced by the single bed system. As has been known CO₂ is

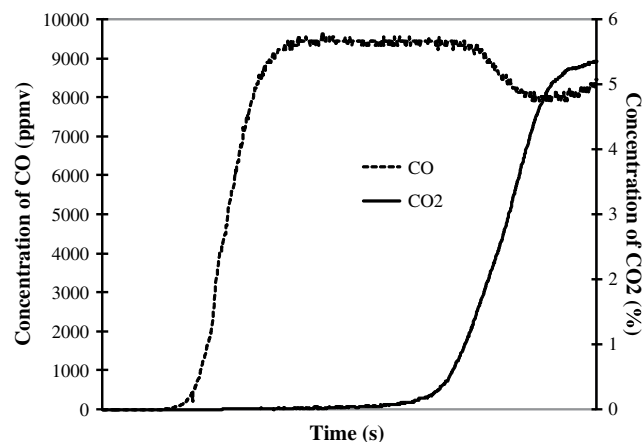


Fig. 4 – Concentration of CO–CO₂ in the adsorption column.

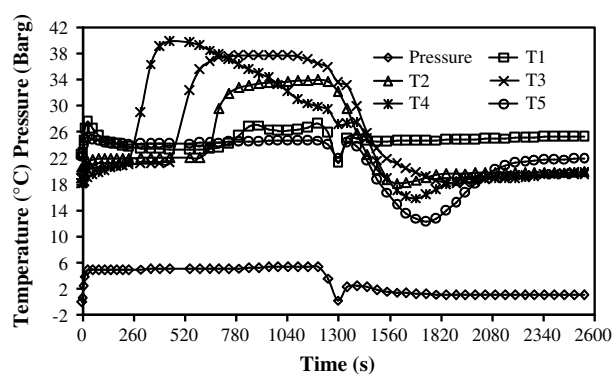


Fig. 5 – The temperature and pressure profile of CO–CO₂ in the adsorption process.

the easiest to be absorbed by activated carbon compared to CO [12–15]. At the time when CO was detected in the product stream, CO₂ was still not detected because it was adsorbed by the activated carbon. Eventually, the CO level dropped off and CO₂ was then detected in the product stream. Fig. 4 shows that, the CO concentration in the product stream was higher than in the feed gas. The activated carbon had a high selectivity for CO₂ compared to CO. During the adsorption, the CO that had been adsorbed to the activated carbon was replaced by CO₂.

There were two processes that could have taken place at the adsorbent layer during adsorption of CO₂. During these processes CO₂ was adsorbed while CO was desorbed from the adsorbent simultaneously. The CO desorption process by CO₂ is indicated by the increase in CO concentration in the product gas stream. When the adsorbent became saturated, the CO concentration decreased to the initial concentration, while the CO₂ concentration increased till it achieved the initial concentration in the feed gas.

The adsorption processes involved two components, namely, the strong and weak adsorption forces, whose concentration history is shown in Fig. 4. A similar observation was made in other investigations on the adsorbates–adsorbent relation such as by Siddiqi et al [16], Motoyuki [17], Kenneth et al [18], Vasdat et al [19], Lavanchy et al [20] and Edy [21].

Fig. 5 shows the temperature history in the adsorption column during the adsorption. The temperature increases from the bottom to the top of the adsorption bed. The temperature increased according to the following sequence: T4 (10 cm from bottom), T3 (20 cm from bottom), and T2 (30 cm from bottom). T1 and T5 were temperatures for the top and the bottom sections of the column (an empty space). The

Table 5 – The average temperature of single adsorption during the CO–CO₂ adsorption process.

Temperature of bed (°C)	T1	T2	T3	T4	T5
Initial temperature	22.79	22.07	21.85	21.19	22.91
Highest temperature	26.95	37.96	39.13	39.27	24.89
Increasing temperature	4.16	15.89	17.28	18.06	1.98

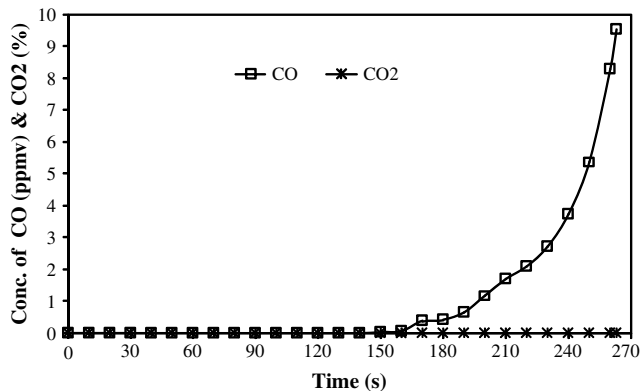


Fig. 6 – The CO–CO₂ concentration profiles in the hydrogen stream.

temperatures at T1 and T5 were the gas temperature at the inlet and outlet, respectively (Fig. 5). Meanwhile, the temperatures at T2, T3 and T4 were the recorded temperatures along the adsorption bed. The highest temperature recorded in the bed was 39.1 °C and the highest average increase of temperature was 18.1 °C (Table 5).

3.2.2. Dual bed cycle

3.2.2.1. Batch adsorption process. The adsorption process was stopped when the CO concentration in the hydrogen product from the second bed reached 10 ppm, and the desorption cycle commenced. In this dual bed adsorption test, the beds used were bed number 3 (Bed 3) and 4 (Bed 4). The gas entered at Bed 3, and then the product from Bed 3 was directed to Bed 4 as a feed gas. The final product was taken from the exit of Bed 4.

Fig. 6 shows the CO and CO₂ concentration profile in the hydrogen product stream from Bed 4. The hydrogen stream did not contain CO and CO₂ until the adsorption process was run for 160 s. After 263 s, the CO concentration in the product stream was 9.5 ppm, while CO₂ was not detected. This shows that CO₂ has been completely adsorbed. Since the concentration of CO was close to the limit required for hydrogen as

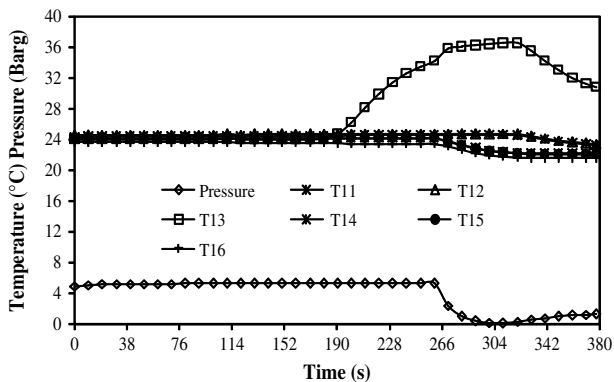


Fig. 7 – Pressure and temperature profile in the adsorption column.

Table 6 – The increase of multiple adsorption temperature during the CO–CO₂ adsorption process.

Temperature of bed (°C)	T11	T12	T13	T14	T15	T16
Initial temperature	24.32	24.51	23.98	24.07	24.10	23.60
Highest temperature	24.60	24.69	36.49	24.13	24.13	23.63
Increasing temperature	0.28	0.18	12.51	0.06	0.03	0.03

PEMFC fuel, the adsorption process was stopped and the bed was regenerated.

The pressure and temperature profiles in the CO–CO₂ adsorption using dual bed adsorption are shown in Fig. 7. The profile shows the pressure during adsorption, decreasing of pressure (blowdown), and cleaning stage (purging). This pressure profile has the same pressure pattern as in the single bed cycle (Fig. 5). The temperature profiles in the dual bed only show an increase in temperature in Bed 3, which is at section T13 (10 cm from bottom). The temperature only increases at the adsorbent layer at the gas feed section due to the heat released during CO₂ adsorption. All CO₂ fed into Bed 3 was completely adsorbed at section T13.

The temperature in Bed 3 is slightly higher compared to Bed 4, during either adsorption or desorption. The highest temperature achieved by Bed 3 was 36 °C and the total temperature increase during the adsorption was 12.51 °C (Table 6).

3.2.2.2. Continuous adsorption. For continuous adsorption, similar feed conditions were used. The adsorption cycle is shown in Fig. 8. Fig. 9 shows the concentration of CO and CO₂ in the hydrogen product stream, which had run for 60 cycles. The CO₂ concentration in the hydrogen stream was 7 ppm. This value is below acceptable fuel specification value of hydrogen stream in PEMFC which is 10 ppm. Therefore, from these 60 cycles, it was shown that CPSA using activated carbon was able to purify hydrogen to the required levels of CO and CO₂ of 1.4 ppm and 7 ppm, respectively. For continuous adsorption, the average hydrogen product purity was 99.999%, product throughput of 0.04 kg H₂/kg adsorbent with purge/feed ratio was 0.001 and vent loss/feed ratio was 0.02.

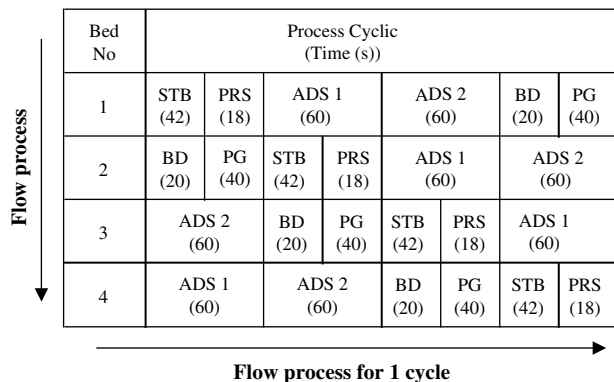


Fig. 8 – Process flow in the CO–CO₂ adsorption process using continuous multiple adsorption.

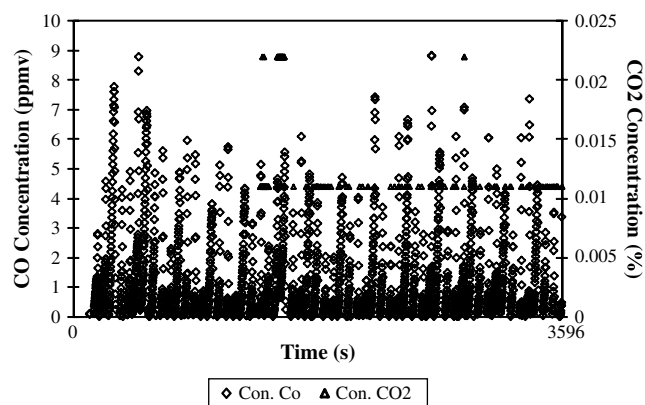


Fig. 9 – Concentration profiles of CO and CO₂ in the hydrogen product stream.

4. Conclusions

Activated carbon from Sigma–Aldrich has been successfully used to adsorb CO. The adsorption capacity was 0.13 mmol CO/g. CPSA was able to reduce the CO concentration in H₂/CO/CO₂ mixture from 4000 ppm to 1.4 ppm and CO₂ from 5% to 7 ppm. For the continuous adsorption, the average hydrogen product purity was 99.999%, product throughput of 0.04 kg H₂/kg adsorbent with purge/feed ratio was 0.001 and vent loss/feed ratio was 0.02. Therefore, it can be concluded that the CPSA system was able to purify hydrogen to the required specifications of hydrogen fuel for PEM fuel cell applications.

Acknowledgment

The authors would like to express their gratitude to the Ministry of Science, Technology and Innovation of Malaysia for the financial support through IRPA grant: IRPA 02-02-02-0001-PR0023 11-06.

REFERENCES

- [1] US DOE. Fuel cell handbook. 5th ed. Morgantown, West Virginia; 2000. p. I-1, I-2, III-11.
- [2] Towler GP, Bussche KV. Control system for providing hydrogen for use with fuel cells. US patent 6280864; 2001.
- [3] Vasiliev LL, Kanonchik LE, Kulakov AG, Mishkinis DA, Safonova AM, Luneva NK. New sorbent materials for the hydrogen storage and transportation. *Int J Hydrogen Energy* 2007;32:5015–25.
- [4] Meuller LF, Tzimas E, Kaltschmitt M, Peteves S. Techno-economic assessment of hydrogen production processes for the hydrogen economy for the short and medium term. *Int J Hydrogen Energy* 2007;32:3797–810.
- [5] Van Keulen ANJ, Reinkingh JG. Hydrogen purification. US patent 6403049; 2002.
- [6] Marcelo T, Gaston D. Optimization of a hydrogen purification system. *Int J Hydrogen Energy* 2008;33:3496–8.
- [7] White Jr H, Barkley PG. The design of pressure swing adsorption systems. *Chem Eng Prog* 1989;85:25–33.
- [8] Regea SU, Yang RT, Qiana K, Buzanowski MA. Air-prepurification by pressure swing adsorption using single/layered beds. *Chem Eng Sci* 2001;56:2745–59.
- [9] Hirai H, Ootsuka N, Sakai K, Shimazawa T. Adsorbent for carbon monoxide. US patent 5922640; 1999.
- [10] Iyuke SE, Daud WRW, Mohamad AB, Kadhum AA, Faisal HZ, Shariff AM. Application of Sn-activated carbon in pressure swing adsorption for purification of H₂. *Chem Eng Sci* 2000; 55:4745–55.
- [11] Al-Khatib MF, Iyuke SE, Abu BM, Wan RWD, Kadhum AAH, Azmi MS, et al. The effect of impregnation of activated carbon with SnCl·2H₂O on its porosity, surface composition and CO gas adsorption. *Carbon* 2002;40:1929–36.
- [12] Yokoe J, Takeuchi M, Tsuji T. Adsorbent for separation-recovery of CO, preparing method thereof and process for separation-recovery of high purity CO, using the adsorbent. US patent 4713090; 1987.
- [13] Tsuji T, Shiraki A, Shimono H. Method of producing an adsorbent for separation and recovery of CO. US patent 4914076; 1990.
- [14] Krishnamurthy R. Hydrogen and carbon monoxide production by hydrocarbon steam reforming and pressure swing adsorption purification. US patent 5096470; 1992.
- [15] Peng XD. CO adsorbents with hysteresis. US patent 5529970; 1996.
- [16] Siddiqi KS, Thomas WJ. The adsorption of methane–ethane mixtures on activated carbon. *Carbon* 1982;20:473–9.
- [17] Motoyuki S. Adsorption engineering. Tokyo: Kodansha Ltd.; 1990.
- [18] Kenneth EN, Vassilios G, Hou WS. Adsorption technology for air and water pollution control. Michigan: Lewis Pub. Inc.; 1992.
- [19] Vasdat N, Swearngen PM, Johnson JS. Adsorption prediction of binary mixtures on adsorbents used in respirator cartridges and air sampling monitors. *AIHA J* 1994;55(10):909–17.
- [20] Lavanchy A, Stoeckli F. Dynamic adsorption of vapour mixtures in activated carbon beds described by the Myers–Prausnitz and Dubinin theories. *Carbon* 1997;35(11):1573–9.
- [21] Edy Herianto Majlan. Adsorption of volatile organic compounds using thermal swing adsorption system. Thesis, Universiti Kebangsaan Malaysia; 2001.